

# Donor-acceptor heterojunction solar cells based on perylene diimide and perylene bisbenzimidazole\*

S. Erten<sup>1,a</sup>, F. Meghdadi<sup>2</sup>, S. Gunes<sup>2</sup>, R. Koeppel<sup>2</sup>, N.S. Sariciftci<sup>2</sup>, and S. Icli<sup>1,b</sup>

<sup>1</sup> Ege University, Solar Energy Institute, 35100, Bornova, Izmir, Turkey

<sup>2</sup> Linz Institute for Organic Solar Cells (LIOS), Physical Chemistry, Johannes Kepler University, 4040 Linz, Austria

Received: 25 July 2006 / Received in final form: 11 October 2006 / Accepted: 17 October 2006

Published online: 10 January 2007 – © EDP Sciences

**Abstract.** We have fabricated heterojunction solar cells comprising active layers of perylene diimide (PDI) or perylene bisbenzimidazole (CONPER, conjugated perylene dye) as electron acceptor and ZnPC as donor. Bilayer solar cells were produced by successive evaporation of zinc phthalocyanine (ZnPC) and perylene diimide (PDI) or perylene bisbenzimidazole (CONPER) on glass substrates coated with indium doped tin oxide. Active layers with different thickness were evaporated. The bilayer cells were characterized under simulated AM 1.5 illumination (100 mW/cm<sup>2</sup>). The best results were obtained for the device structure of ITO/PEDOT/ZnPC (40 nm)/perylene bisbenzimidazole (60 nm)/Al (70 nm).

**PACS.** 70. Condensed matter: electronic structure, electrical, magnetic, and optical properties – 73.50.Pz Photoconduction and photovoltaic effects

## 1 Introduction

Thin films of organic dyes contain conjugated  $\pi$ -electron systems are widely used in electronic and optoelectronic devices such as organic light-emitting diodes, solar cells and transistors [1–9]. The emerging field of organic semiconductor materials and devices is extending the possibilities of modern electronics into high volume, low cost domains. Among the potentially most significant devices studied are photovoltaic (PV) cells and, organic photodetectors (PDs) [10]. Solid state organic solar cells have attracted much interest because of the motivation for developing inexpensive, efficient and renewable energy sources [11,12]. As materials for organic solar cells, perylene dyes have attracted much attention due to their high thermal and chemical stabilities, and excellent photoconductive properties [13–16].

Phthalocyanines are promising materials for heterojunction solar cells because of their high stability and photoconductivity. Perylene diimide or perylene bisbenzimidazole covers the visible spectrum and find applications in the fields of photovoltaic cells, optical switches, lasers, organic light emitting diodes [17–23].

In this work, we report the synthesis and device characterizations of perylene bisbenzimidazole (conjugated perylene, CONPER) and N,N'-bis-dehydroabietyl-3,4,9,10-perylene diimide (PDI). We have produced het-

erogunction solar cells by using the dyes of phthalocyanine as electron donor (hole transport material), and perylene diimide (PDI) or perylene bisbenzimidazole (CONPER) as electron acceptor (electron transport material). Molecular structures of used materials are presented in Figure 1. We investigated absorptions, thermal stabilities, electrochemical behaviors of these two dyes before fabrication of solar cells. PDI and CONPER have different molecular structures and absorption spectra. PDI (red dye) shows strong absorption in the range of 425–550 nm. Whereas, perylene bisbenzimidazole (navy blue dye) absorbs the all visible region (350–800 nm) because of the extended conjugation in the molecular structure. Thermal gravimetric analysis showed that they are stable up to 400 °C. Fabrication of the bilayer heterojunction solar cells were done using different thicknesses of ZnPC and PDI or CONPER and photovoltaic characteristics of bilayer cells were investigated. The current-voltage (*I-V*) characteristics of the bilayer cells were measured under simulated AM 1.5 illumination (100 mW/cm<sup>2</sup>). Heterojunction solar cells consisting of different active layer thicknesses show different cell characteristics based on the role of each organic layer in these bilayer devices.

## 2 Experimental section

### 2.1 Synthesis of perylene bisbenzimidazole and perylene diimide

All used reagents were commercial grade and used without any further purification. Perylene bisbenzimidazole and

\* This paper has been presented at “ECHOS06”, Paris, 28–30 juin 2006.

<sup>a</sup> e-mail: [sule.erten@ege.edu.tr](mailto:sule.erten@ege.edu.tr)

<sup>b</sup> e-mail: [siddik.icli@ege.edu.tr](mailto:siddik.icli@ege.edu.tr)

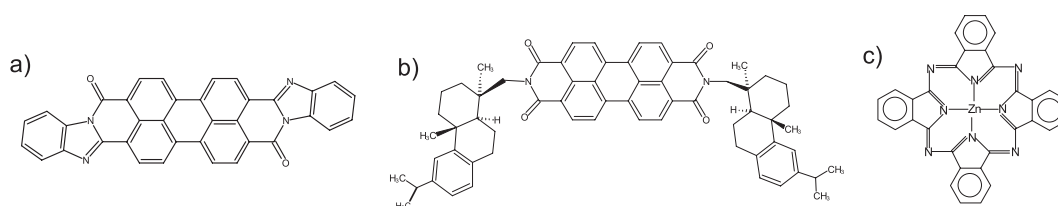


**Fig. 1.** Molecular structure of used materials, (a) Perylene bisbenzimidazole, CONPER (b) *N,N'*-bis-dehydroabietyl-3,4,9,10-perylene diimide, PDI (c) Zinc phthalocyanine, ZnPC.

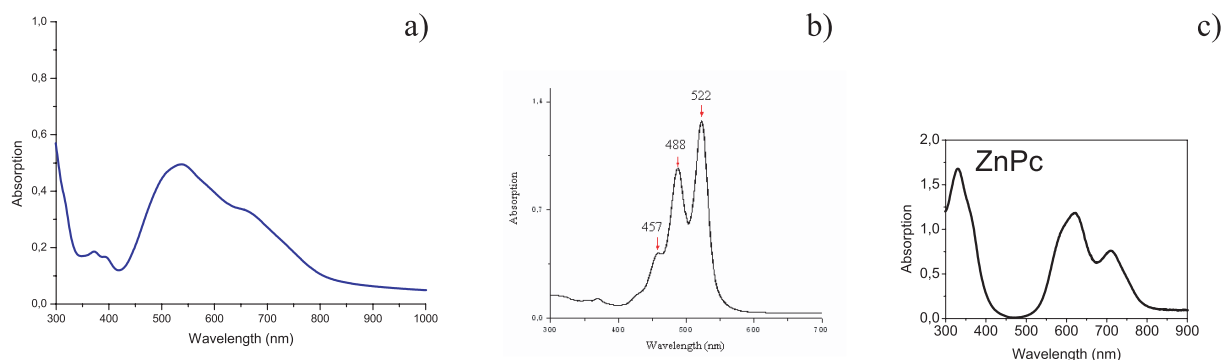


**Fig. 2.** Absorption spectra of perylene bisbenzimidazole, CONPER (a), *N,N'*-bis-dehydroabietyl-3,4,9,10-perylene diimide, PDI (b), Zinc phthalocyanine, ZnPC (c).

perylene diimide were synthesized by condensation reaction of alkyl (aryl) amine and perylene dianhydride in imidazole as solvent. Molecular structure was identified by using IR,  $^1\text{H}$  NMR spectrophotometer. Zinc phthalocyanine, ZnPC, was purchased from Fluka.

IR data of perylene bisbenzimidazole, CONPER, (KBr),  $\text{cm}^{-1}$ , 3053, 1679, 1654, 1590, 1541, 1500, 1446, 1387, 1355, 1293, 1284, 1236, 1185, 1158, 1080, 984, 886, 842, 806, 748, 644.  $^1\text{H}$  NMR data,  $\delta$  (ppm), 8.39(2H), 8.83(2H), 8.31(2H), 8.30(2H), 7.85(2H), 7.40(2H), 7.70(2H), 7.63(2H), 7.2( $\text{CDCl}_3$ ), 11( $\text{CF}_3\text{COOH}$ ).

IR data of *N,N'*-bis-dehydroabietyl-3,4,9,10-perylene diimide, PDI, (KBr); ( $\text{cm}^{-1}$ ) 2950, 2900, 2850, 1707, 1666, 1580, 1495, 1380, 1315, 1445, 1245, 1160, 1050, 980, 880, 810, 765.  $^1\text{H}$  NMR ( $\text{CDCl}_3$ ):  $\delta$  (ppm), 8.40(4H), 8.47(4H), 7.33(2H), 7.19(2H), 7.03(2H), 4.33(4H), 2.9(2H), 1.4-1.5(2H), 1.4-1.5(20H), 2.8(12H), 1.6(12H).

## 2.2 Electrochemical measurements for perylene bisbenzimidazole and perylene diimide

Cyclic Voltammetry (CV), measurements of perylene bisbenzimidazole and *N,N'*-bis-dehydroabietyl-3,4,9,10-perylene diimide were taken by using CH-Instrument 660 B Model Potentiostat equipment. A three electrode cell was used consisting of Glassy carbon working electrode, Pt wire counter electrode and Ag/AgCl reference electrode. Ferrocene was used as internal reference electrode. Tetra-butylammonium hexafluorophosphate ( $\text{TBAPF}_6$ ), was supporting electrolyte (0.1 M). All measurements were recorded under inert atmosphere.

## 3 Results and discussion

### 3.1 Absorption and electrochemical properties of dyes

Perylene diimides absorb in the visible region of solar spectrum [24, 25, 27]. *N,N'*-bis-dehydroabietyl-3,4,9,10-perylene diimide, PDI, shows strong absorption in the range of 425–550 nm. UV absorption spectrum of perylene diimide gives three characteristic bands at 457, 488 and 522 nm in Figure 2b. The selection of dehydroabietyl substituent on perylene diimide, is based on the predictions that a bulky condensed cycloalkyl moiety would prevent the aggregation and inter-molecular interactions, as a result photo-electron transfer processes would be enhanced in photo-electronic devices. The presence of conjugated groups attached to the perylene moiety are also critical, because these substituents alter the absorption and emission toward higher wavelength region which result in enhanced absorption of solar spectrum. Phenylene group, condensed on to the perylene diimide ring causes a pronounced red shift (bathochromic effect of 138 nm with respect to PDI). Two characteristic bands at 530 and 660 nm of CONPER are seen in Figure 2a. Announced bathochromic effect alters also the photophysical and electrochemical properties of the CONPER dye. Perylene bisbenzimidazole, CONPER, covers nearly all of the visible region of solar spectrum owing to extended conjugation. ZnPC absorbs the light in the range of 300–400 and 510–800 nm in Figure 2c. CONPER/ZnPC and PDI/ZnPC in bilayer devices thus are expected to absorb the whole visible region of solar spectrum.

We calculated the band gap values,  $E_g$ , of the CONPER and PDI dyes by cyclic voltammetry measurements.

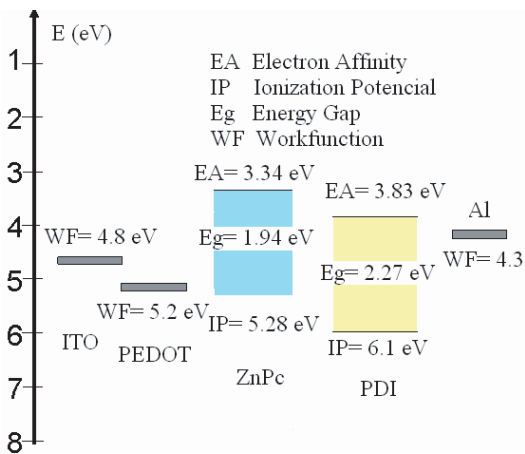


**Fig. 3.** Schematic energy diagram for the device of ITO/PEDOT/ZnPC/PDI dye/Al.

In literature, the band gap,  $E_g$ , of perylene bisbenzimidazole, CONPER, is given as  $<1.7$  eV [20,28,29]. Our calculations are consistent with the literature. The band gap,  $E_g$ , values are calculated as 1.5 eV for perylene bisbenzimidazole, CONPER, and 2.27 eV for N,N'-bis-dehydroabietyl-3,4,9,10-perylene dimide, PDI. Schematic energy diagram in Figure 3 presents work function,  $WF$ , electron affinity,  $EA$ , ionization potential,  $IP$ , and band gap energy values,  $E_g$ , for ITO, PEDOT, ZnPC, PDI and Al which are placed in ITO/PEDOT/ZnPC/PDI dye/Al device. Photoexcited ZnPC transfers the electron to aluminium layer via PDI dye, PEDOT acts as hole conductor in ITO/PEDOT/ZnPC/PDI dye/Al device.

### 3.2 Thermal stabilities of dyes

Perylene diimides are known to be thermal and photo-stable materials [25–27]. Thermal stability is determined by means of thermal gravimetry, TGA, measurements. The dyes to be employed in solar cells, must have high thermal- and photostabilities under illumination conditions. Dyes that degrade easily under solar irradiation conditions can not be employed in photo-electronic devices.

TGA curves of perylene derivatives are presented in Figures 4, 5. PDI and CONPER dye are stable up to 400 °C. Decomposition temperatures initiates from 425 °C and ends at 530 °C. PDI and CONPER are versatile molecules and excellent photosensitizers based on their thermal and photostabilities. Perylene diimides were employed as photosensitizers concentrated sun light for the photosynthesis of fine chemicals, solar photodegradations and in solar cell fabrications [19,25–27].

### 3.3 Photovoltaic performance of heterojunction solar cell based on PDI and CONPER dyes

The photovoltaic characterization of bilayer heterojunction solar cells based on CONPER and PDI dye were determined by measuring  $I-V$  (current-voltage)

curves in the dark and under illumination (AM 1.5, 100 mW/cm<sup>2</sup>) through the ITO-PEDOT:PSS side. Current density-voltage characteristics in dark and under illumination were presented in semilogarithmic and linear scales for CONPER dye in Figure 7. The active layers were evaporated in different thicknesses. Structure of bilayer heterojunction device is presented in Figure 6. For these experiments, we fixed the PDI layer as 30 nm. We changed the thickness of the ZnPC layer to determine the best thickness of donor layer. We prepared different device structures; device I, ITO/PEDOT/ZnPC(20 nm)/PDI(30 nm)/Al(70 nm); device II, ITO/PEDOT/ZnPC(40 nm)/PDI(30 nm)/Al(70 nm); device III, ITO/PEDOT/ZnPC(60 nm)/PDI(30 nm)/Al(70 nm). We obtained the best result for device II; ITO/PEDOT/ZnPC(40 nm)/PDI(30 nm)/Al(70 nm). We obtained the cell characteristics of device II as  $V_{oc} = 0.55$  V,  $J_{sc} = 0.9$  mA/cm<sup>2</sup>,  $FF = 0.25$ ,  $\eta = 0.12\%$ . We repeated the same operations for the perylene bis benzimidazole dye. In Figure 7, red  $I-V$  Curve (device V), Black  $I-V$  curve (device IV) and Blue  $I-V$  curve (device VI) belong to the device structures of ITO/PEDOT/ZnPC(40 nm)/CONPER(60 nm)/Al(70 nm); ITO/PEDOT/ZnPC(40 nm)/CONPER(40 nm)/Al(70 nm); ITO/PEDOT/ZnPC(40 nm)/CONPER(80 nm)/Al(70 nm), respectively. Table 1 shows the summary of photovoltaic properties of different device structures for CONPER dye. Selected thicknesses of ZnPC(40 nm)/CONPER (60 nm) is same as for ZnPC/PDI dye device structure. Lower (20 nm) and higher (60 nm) thicknesses of ZnPC layer show negative effects. The thickness of ZnPC layer gives the best result at 40 nm. All over best results were obtained in the device structure of ITO/PEDOT/ZnPC(40 nm)/CONPER(60 nm)/Al(70 nm). In all of the devices (device IV–VI)  $V_{oc}$ , 0.48 V, and  $FF$ , 0.52–0.56, are seen to be similar. But short circuit current density and power conversion efficiency of the device V,  $\eta = 1.3$ , is higher with respect to the corresponding values of devices IV and VI,  $\eta = 0.7$  and  $\eta = 0.4$ , respectively. The cell characteristics of all devices are listed in Table 1. Figure 7 shows incident photon to current efficiency (IPCE) spectra for device-IV, device-V and device-VI. Device structure with ITO/PEDOT/ZnPC(40 nm)/CONPER(60 nm)/Al(70 nm) gave the best IPCE spectrum.

## 4 Conclusion

A comparative study on absorption spectra, electrochemistry, thermal stabilities, photovoltaic performances of two dyes of perylene bisbenzimidazole, CONPER, and N,N'-bis-dehydroabietyl-3,4,9,10-perylene dimide, PDI, are presented. Thickness dependence on

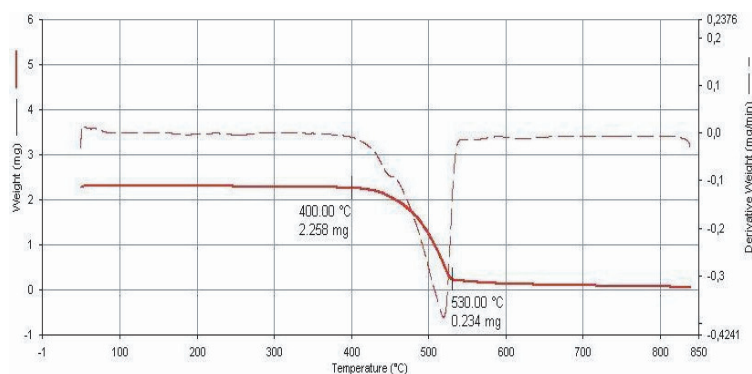


**Fig. 4.** TGA curve of N,N'-bis-dehydroabietyl-3,4,9,10-perylene diimide, PDI.

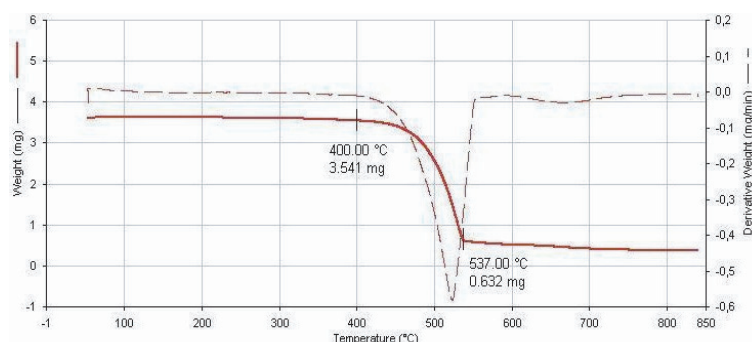


**Fig. 5.** TGA curve of perylene bisbenzimidazole, CONPER.

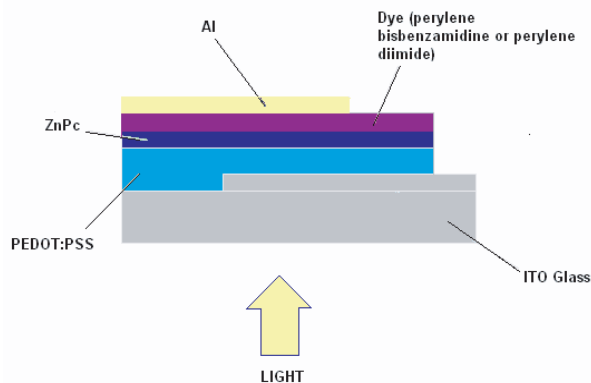


**Fig. 6.** Structure of bilayer heterojunction device.

the performance of active layer in bilayer heterojunction solar cells was investigated. The best result is obtained at power conversion efficiency of 1.3% for device ITO/PEDOT/ZnPC(40 nm)/CONPER (60 nm)/Al (70 nm). The active layer thicknesses are thought to determine the number of absorbed photons in the active region of bilayer heterojunction solar cells, and thus thicknesses of each layer are critical parameters.

This work has been performed within the European Unions STREP Project MOLYCELL. We acknowledge the help of LIOS members, Konarka-Austria group and the Project

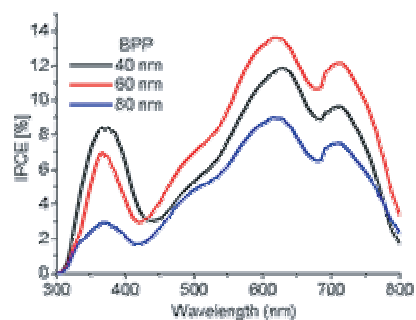
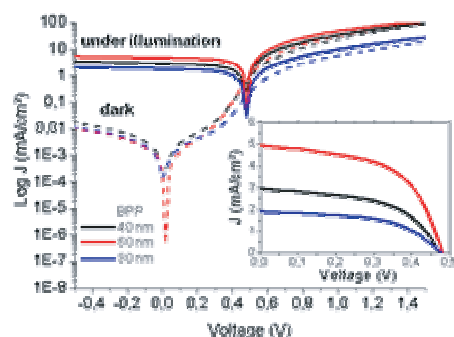


**Fig. 7.** Current density-voltage characteristics in dark and under illumination for device IV–VI, ITO/PEDOT/ZnPC(40 nm)/CONPER(40, 60, 80 nm)/Al(70 nm) and short circuit photocurrent spectra, IPCE for the device of ITO/PEDOT/ZnPC/CONPER/Al with different thicknesses of active layers.

**Table 1.** Summary of the photovoltaic properties for the devices of ITO/PEDOT/ZnPC(40 nm)/CONPER(40, 60, 80 nm)/Al(70 nm),  $D_{\text{CONPER}}$ ; thickness of CONPER  $J_{sc}$ ; short circuit current density,  $V_{oc}$ ; open circuit voltage,  $FF$ ; filling factor and  $\eta$ ; power conversion efficiency.

	$D_{\text{CONPER}}$ [nm]	$J_{sc}$ [mA/cm <sup>2</sup> ]	$V_{oc}$ [V]	$FF$	$\eta$ [%]
Device IV	40	2.9	0.47	0.54	0.7
Device V	60	4.9	0.48	0.56	1.3
Device VI	80	1.9	0.48	0.52	0.4

support funds of Scientific Research Council of Turkey (TUBITAK, TBAG\_106T061).

## References

1. C.W. Tang, Appl. Phys. Lett. **48**, 183 (1986)
2. C.J. Brabec, N.S. Sariciftci, J.C. Hummelen, Adv. Funct. Mater. **11**, 15 (2001)
3. M.T. Bernius, M. Inbasekaran, J. O'Briben, W. Wu, Adv. Mater. **12**, 1737 (2000)
4. Y.Z. Wang, R.G. Sun, D.K. Wang, T.M. Swager, A. Epstein, Appl. Phys. Lett. **74**, 2593 (1999)
5. J. Rostalski, D. Meissner, Sol. Energ. Mat. Sol. C. **61**, 87 (2000)
6. M. Westphalen, U. Kreibig, J. Rostalski, H. Lüth, D. Meissner, Sol. Energ. Mat. Sol. C. **61**, 97 (2000)
7. K. Takahashi, N. Kuraya, T. Yamaguchi, T. Komura, K. Murata, Sol. Energ. Mat. Sol. C. **61**, 403 (2000)
8. M. Pfeiffer, A. Beyer, B. Plönnigs, A. Nollau, T. Fritzz, K. Leo, D. Schlettwein, S. Hiller, D. Wöhrle, Sol. Energ. Mat. Sol. C. **63**, 83 (2000)
9. M. Hoffmann, K. Schmidt, T. Fritz, T. Hasche, V.M. Agranovich, K. Leo, in *Multiphoton and Light Driven Multielectron Processes: Materials, Phenomena, Applications*, edited by F. Kajzar, V. Agranovich (NATO Advanced Research Workshop, Kluwer, Dordrecht, the Netherlands, 2000), p. 123
10. P. Peumans, A. Yakimov, S.R. Forrest, J. Appl. Phys. **93**, 7 (2002)
11. T.U. Kampen, G. Gavrila, H. Mendez, D.R.T. Zahn, A.R. Vearey-Roberts, D.A. Evans, J. Wells, I. IMcGovern, W. Braun, J. Phys.-Condens. Matter **15**, 2679 (2003)
12. G. Yu, J. Gao, J.C. Hummelen, F. Wudl, A.J. Heeger, Science **270**, 1789 (1995)
13. M. Grandström, K. Petritsch, A.C. Arias, A. Lux, M.R. Andersson, R.H. Friend, Nature **395**, 258 (1998)
14. C.C. Leznoff, *Phthalocyanines, Properties and Applications* (VCH, New York, 1989)
15. M. Hiramoto, H. Fujiwara, M. Yokoyama, Appl. Phys. Lett. **58**, 1062 (1991)
16. M. Hiramoto, H. Fukusumi, M. Yokoyama, Appl. Phys. Lett. **61**, 2580 (1992)
17. H. Quante, Y. Geerts, K. Müllen, Chem. Mater. **9**, 495 (1997)
18. S. Erten, F. Meghdadi, S. Gunes, N.S. Sariciftci, S. Icli, in *XIX. National Chemistry Conference, Kusadasi, Turkey, 30 September-4 October, 2005*
19. H. Dincalp, S. Icli, J. Photochem. Photobiol: A Chem. **141**, 147 (2001), H. Dincalp, S. Icli, Sol. Energ. **80**, 332 (2006)
20. W. Hu, M. Matsumura, J. Phys. D Appl. Phys. **37**, 1434 (2004)
21. J.C. Scott, J. Vac. Sci. Technol. A **21**, 521 (2003)
22. J. Nelson, J. Kirkpatrick, P. Ravirajan, Phys. Rev. B **69**, 035337 (2004)
23. V.P. Singh, O.M. Erickson, J.N. Chao, J. Appl. Phys. **78**, 4538 (1995)
24. B. Maennig, J. Drechsel, D. Gebeyehu, P. Simon, F. Kozłowski, A. Werner, F. Li, S. Grundmann, S. Sonntag, M. Koch, K. Leo, M. Pfeiffer, H. Hoppe, D. Meissner, N.S. Sariciftci, I. Riedel, V. Dyakonov, J. Parisi, Appl. Phys. A Mater. **79**, 1 (2004)
25. Th. B. Singh, S. Erten, S. Gunes, C. Zafer, G. Turkmen, B. Kuban, Y. Teoman, N.S. Sariciftci, S. Icli, Org. Electron. **7**, 480 (2006); S. Erten, *Photochemical actinometry studies under concentrated sun light*, Ph.D. Thesis, Ege University, Solar Energy Institute, Izmir, Turkey, 2004
26. B.A. Gregg, M.A. Fox, A.J. Bard, J. Am. Chem. Soc. **111**, 3024 (1989)
27. B.A. Gregg, Chem. Phys. Lett. **258**, 376 (1996)
28. W.L. Yu, Y. Cao, J. Pei, W. Huang, A.J. Heeger, Appl. Phys. Lett. **75**, 3270 (2000)
29. I.G. Hill, J. Schwartz, A. Kahn, Org. Electron. **1**, 5 (2000)